

# Thermoelectric properties of nanocomposite Bi<sub>2</sub>Te<sub>3</sub> layers prepared by PLD

R. Zeipl<sup>\*</sup>, M. Jelínek<sup>\*</sup>, M. Vlček<sup>\*\*</sup>, T. Kocourek<sup>\*</sup>, J. Remsa<sup>\*</sup> and J. Vaníš<sup>\*\*\*</sup>

<sup>\*</sup>Institute of Physics of the Academy of Sciences of the Czech Republic, v.v.i., Na Slovance 2, 18221 Prague, Czech Republic, zeipl@fzu.cz

<sup>\*\*</sup>Institute of Macromolecular Chemistry of the Academy of Sciences of the Czech Republic, v.v.i., Heyrovského nám. 2, 16206 Prague, Czech Republic, milan.vlcek@upce.cz

<sup>\*\*\*</sup>Institute of Photonics and Electronics of the Academy of Sciences of the Czech Republic, v.v.i., Chaberská 57, 18251 Prague, Czech Republic, vanis@ufe.cz

## ABSTRACT

Some properties of thermoelectric nano-layers prepared by Pulsed Laser Deposition prepared from Bi<sub>2</sub>Te<sub>3</sub> target are presented. The layers were prepared under various deposition conditions to study its influence on the quality of the surface. Crystallinity, composition and morphology of the layers are presented. Nano crystallites observed on the layer's surface are studied by X-ray Diffraction and by Atomic Force Microscope. Results, comparison and experiences are discussed.

**Keywords:** thermoelectric materials, thin layers, pulsed laser deposition

## 1 INTRODUCTION

Thin layers and multi-layered thermoelectric structures are potential candidates for many thermoelectric applications and nano devices from solid-state coolers and generators, thermoelectric transducers, thermocouples to thermal sensors and detectors.

A relative efficiency of thermoelectric material is expressed in terms of the dimensionless figure of merit (ZT). It depends on the Seebeck coefficient, the electrical conductivity, the thermal conductivity and on the absolute temperature. Despite of no theoretical ZT limit, it seems that ZT of about 1 is a practical limit for a majority of conventional thermoelectric materials [1, 2]. Bismuth and tellurium compounds, such as Bi<sub>2</sub>Te<sub>3</sub> etc., prepared in a form of very thin layers (nano layers) have been well established candidates for many thermoelectric applications.

Knowledge of thermoelectric properties of materials with lateral resolution of tens of nanometres is necessary and the problem of accurate characterization of materials for thermoelectric nano devices is extremely important from the nano physics, nano electronics, nano mechanics and nano medicine point of view of.

We have been working on the development of a simple and reliable method for relative thermal conductivity characterization of thin thermoelectric layers and multi-layered structures using a scanning thermal microscope

working in constant current active DC and AC modes already for some time. For our experiments we need high quality thermoelectric layers and nano layers with thermal conductivity in the range from about one-tenth to few tens of Wm<sup>-1</sup>K<sup>-1</sup> with a very smooth surface. The increased surface roughness might cause inaccuracy and create difficulties such as artefacts etc., when using any scanning probe microscope measurement technique, including thermal microscope.

As a suitable thermoelectric material for our experiments we have chosen Bi<sub>2</sub>Te<sub>3</sub> nano layers which were successfully prepared by several deposition methods including Pulsed Laser Deposition (PLD) in the past [3-6].

In this paper we present the influence of the main deposition conditions that include the substrate temperature (T<sub>S</sub>) and the laser beam density (D<sub>S</sub>) on the quality of layer surface. The X-ray Diffraction (XRD) patterns, the Wavelength Dispersive analysis (WDX) and the Energy Dispersive X-ray analysis (EDX) composition and the Atomic Force Microscope (AFM) surface morphology of the prepared layers are presented.

## 2 LAYERS PREPARATION AND MEASUREMENTS

To study the influence of PLD deposition conditions on the resulting layer surface quality with the goal to find the conditions providing the smoothest surface, two series of layers with thickness ranging from 230 nm to 500 nm were prepared on Si (100) substrates from a Bi<sub>2</sub>Te<sub>3</sub> target. The first series layers were prepared at the substrate temperature T<sub>S</sub>=360 °C applying various laser beam density D<sub>S</sub> (1, 2, 3, 4 and 5 Jcm<sup>-2</sup>). The original choice of T<sub>S</sub> was selected based on previously published experiments providing smooth and crystalline Bi<sub>2</sub>Te<sub>3</sub> layers [7, 8]. The second series layers were prepared with different T<sub>S</sub> (200 °C, 250 °C, 300 °C and 400 °C) applying the same D<sub>S</sub>=3 Jcm<sup>-2</sup>, which was chosen based on results observed on the first series layers.

The starting polycrystalline Bi<sub>2</sub>Te<sub>3</sub> material was synthesized from Bi and Te elements of 5N purity in evacuated silica ampoules at 1073 K for 48 hours. After verification of homogeneity of the prepared compound by

means of X-ray powder diffraction, the polycrystalline ingot was crushed using an agate mortar and sieved to obtain particle size below 100  $\mu\text{m}$ . The targets for PLD deposition of 20 mm in diameter and of 2 mm in height were prepared by the hot pressing method (temperature 500  $^{\circ}\text{C}$ , pressure  $\sim 60$  MPa for 1 hour). The measured density of pressed targets reached about 96-98 % of the theoretical density.

The powder X-ray diffraction patterns of the  $\text{Bi}_2\text{Te}_3$  compound used for the target were collected in the Bragg-Brentano geometry on the Bruker D8 Advance diffractometer equipped with a secondary graphite monochromator.  $\text{CuK}\alpha$  radiation was used. The XRD spectrogram of the PLD target compound is depicted in Fig. 1.

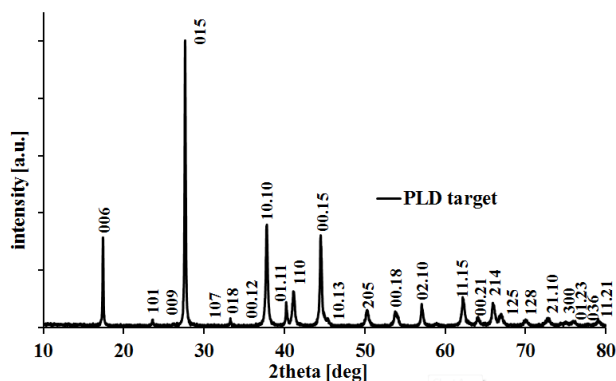


Figure 1: The XRD spectrogram of the PLD target with only peaks corresponding  $\text{Bi}_2\text{Te}_3$  compound.

The basic schema of the experimental apparatus for PLD is depicted in Fig. 2. Conceptually and experimentally, PLD is an extremely simple method, probably the simplest of all the thin film growth techniques. A high power pulsed excimer KrF laser (COMPexProTM 205 F) radiation (1) is used as an external energy source to vaporize materials of the target (5) and to deposit a thin film. A set of optical components is utilized to focus the laser beam on the target surface (2, 3). After the laser pulse irradiation the temperature rises very rapidly ( $10^{11}$  Ks $^{-1}$ ) and the evaporation becomes non-equilibristic. For our experiments the substrates were cleaned from mechanical dirt in an ultrasonic cleaner. Next the substrates were subsequently cleaned in ethyl alcohol, acetone and toluene. Cleaning in vapours of boiling ethyl alcohol then completed the process. A Si (100) wafer was cut on approximately 10x10 mm square shaped substrates. The substrates were finally annealed in an oven at a temperature of around 250  $^{\circ}\text{C}$ . Deposition took place in Ar atmosphere (13 Pa), the target to substrate distance was set to 40 mm and the base vacuum of the coating system was  $5 \times 10^{-3}$  Pa. The layers were prepared by PLD using a KrF excimer laser  $\lambda = 248$  nm,  $\tau = 20$  ns, repetition rate of 10 Hz and laser spot  $2 \times 1$  mm $^2$ .

Thickness and roughness of the layers were measured by an Alpha-step IQ mechanical profilometer (KLA TENCOR Co.). The uncertainty in the thickness estimation is about 10 % in the examined range of thicknesses partly the fact that the layer thickness in the centre of the sample is higher than at its edge.

The layer roughness and homogeneity were characterized by the Atomic Force Microscope (AFM) Solver NEXT (NT-MDT) operating in dynamic regime with HA\_NC tips and in contact mode with CSG10 tips. The layers surface parameters were calculated from a  $50 \times 50$   $\mu\text{m}$  area with software NOVA PX.

The layer composition was studied by the Wavelength Dispersive analysis (WDX) and the Energy Dispersive X-ray analysis (EDX). The analyses were conducted using X-ray JXA-733 micro-analyser JEOL equipped by wavelength dispersive X-ray spectrometers plus in addition an energy dispersive X-ray spectrometer SAMx. As a reference monocrystal  $\text{Bi}_2\text{Te}_3$  was used.

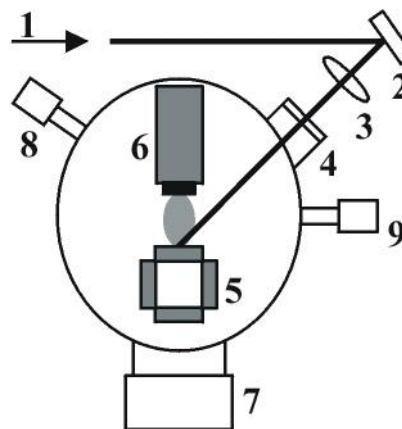


Figure 2: The basic scheme of PLD apparatus: (1) laser beam, (2) mirrors, (3) focusing lens, (4) quartz window, (5) target holder, (6) substrate holder, (7) vacuum pump, (8,9) Pirani and Penning vacuum gauges, respectively.

### 3 RESULTS AND DISCUSSION

The Energy Dispersive X-ray analysis (EDX) and the Wavelength Dispersive X-ray analysis (WDX) were performed on several layers prepared at  $T_s = 360$   $^{\circ}\text{C}$  applying  $D_s = 5$  Jcm $^{-2}$  to obtain information on layer stoichiometry. The excess of Bi (Bi/Te ratio  $\sim 0.76$ ) in comparison to the PLD target  $\text{Bi}_2\text{Te}_3$  stoichiometry (Bi/Te ratio  $\sim 0.67$ ) was observed in all explored layers. The standard deviation was found to be  $\pm 1.5\%$ . Different deposition conditions or a different target would have to be selected to get the exact  $\text{Bi}_2\text{Te}_3$  stoichiometry, which is not necessary in our experiment. Our goal was to prepare thermoelectric layers with the smoothest possible surface. Thus, more valuable for us was the observation of a very granular surface covered with crystals of different dimensions.

The surface roughness of all prepared layers was studied by AFM (scanned area 50x50  $\mu\text{m}$ ) and checked by Alpha-step mechanical profilometer. The results of these measurements are summarized in table 1.

Deposition condition		Layer thickness [nm]	Profilometer	AFM	
$T_s$ [ $^{\circ}\text{C}$ ]	$D_s$ [ $\text{Jcm}^{-2}$ ]		$S_a$ ( $R_a$ ) [nm]	$S_a$ ( $R_a$ ) [nm]	$S_q$ (RMS) [nm]
360	5	271	1.62	8.76	11.23
360	4	309	1.86	9.81	12.71
360	3	329	1.61	7.72	10.13
360	2	311	1.77	9.46	12.95
360	1	494	10.47	not measurable	
400	3	321	10.82	56.93	38.64
300	3	293	1.76	9.01	6.4
250	3	302	0.97	7.65	5.31
200	3	226	0.84	3.9	2.91

Table 1: The comparison table of surface roughness  $S_a$  ( $R_a$ ) and its RMS value for each prepared nano layer measured by Alpha-step mechanical profilometer.

Generally there are two types of objects observed on the layer's surface. The first are regularly shaped crystals of  $\text{Bi}_2\text{Te}_3$  or  $\text{Bi}_{(2+N)}\text{Te}_{(3+M)}$  compounds ranging in size from about 100 nm to 500 nm. These create a basic surface and were proved to be crystalline by the XRD measurement. Usually crystals peak less than 200 nm above the surface, as seen in the 3D surface visualization depicted in the fig. 5. The second are so called PLD droplets. They are much more spread over the surface and are much less frequent in comparison to the first type. The problem is that they are unfortunately much larger. Their height reaches 400 nm and their diameter is in the range of 200 nm to 300 nm.

The influence of the laser beam density on the surface roughness appears to be negligible, however the smoothest surface was observed applying  $D_s=3 \text{ Jcm}^{-2}$  (see fig. 3).

The impact of the substrate temperature is more important (see fig. 3). With increased  $T_s$  the layers become rougher. This was obvious and visible by eye for the layer prepared at  $T_s=400 \text{ }^{\circ}\text{C}$ . This layer had a different colour (matt white) in comparison to the other layers which are usually silver and shiny. The same trend of dependencies was observed using AFM as well as a mechanical profilometer (see fig. 3 and fig.4). The resulting values are different which expected, due to the use of different methods with varying accuracy.

In general the prepared layers were homogeneous from a macro point of view (the AFM scans were performed in

several different positions over the whole surface and the roughness and granularity remains the same).

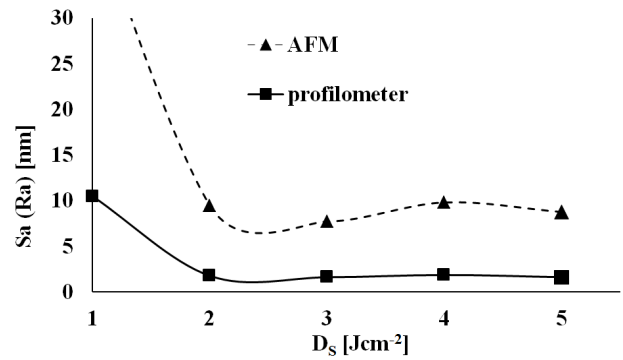


Figure 3: The layer roughness  $S_a$  ( $R_a$ ) versus laser beam density  $D_s$  for samples prepared at the same substrate temperature  $T_s=360 \text{ }^{\circ}\text{C}$ .

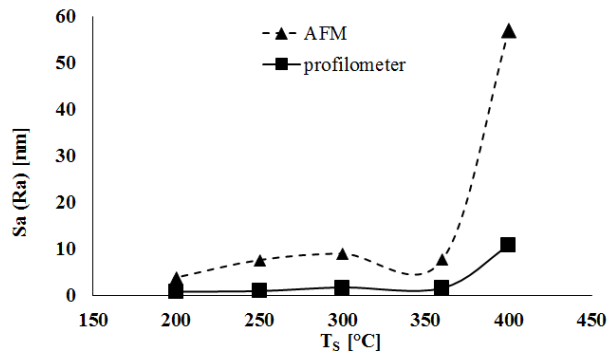


Figure 4: The layer roughness  $S_a$  ( $R_a$ ) versus substrate temperature  $T_s$  for samples prepared applying the same laser beam density  $D_s=3 \text{ Jcm}^{-2}$ .

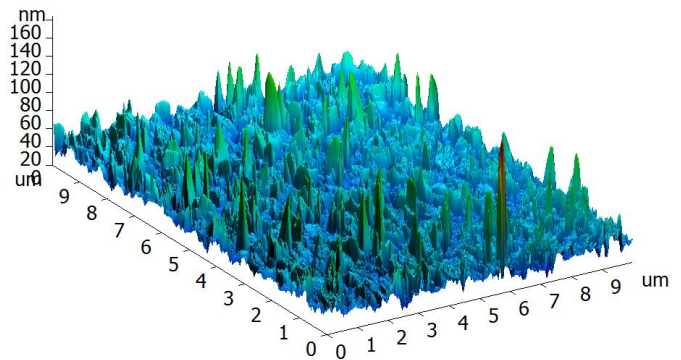


Figure 5: AFM 3D surface visualization of the surface (detail area 10x10  $\mu\text{m}$ ) of the layer prepared at  $T_s=300 \text{ }^{\circ}\text{C}$  applying  $D_s=3 \text{ Jcm}^{-2}$  where crystals and droplets peaking over the surface are visible.

The smoothest layer surface was obtained at  $T_S=200\text{ }^\circ\text{C}$  applying  $D_S=3\text{ Jcm}^{-2}$  is depicted in fig. 6. The roughest measurable layer prepared at  $T_S=360\text{ }^\circ\text{C}$  applying  $D_S=4\text{ Jcm}^{-2}$  is shown in fig. 7. The layer prepared at  $T_S=360\text{ }^\circ\text{C}$  applying  $D_S=1\text{ Jcm}^{-2}$  was not measurable at all. It is important to emphasise that these deposition conditions might not be optimal from thermoelectric properties point of view, as they influence the layer stoichiometry.

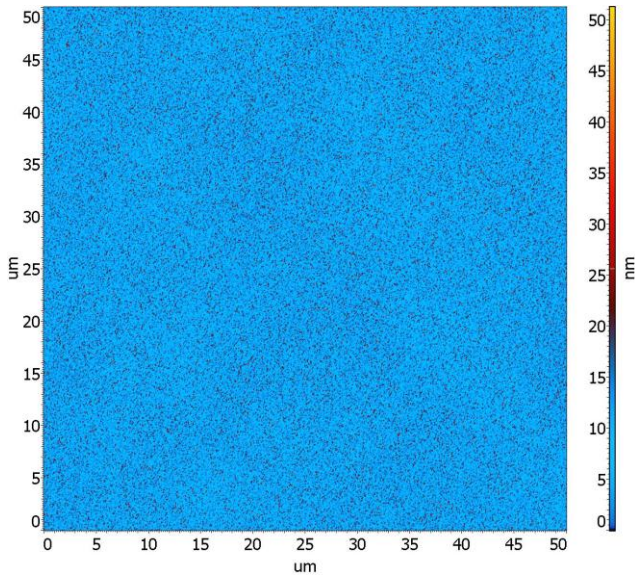


Figure 6: AFM surface morphology (scanned area  $50\times 50\text{ }\mu\text{m}$ ) of the smoothest nano layer prepared at  $T_S=200\text{ }^\circ\text{C}$  applying  $D_S=3\text{ Jcm}^{-2}$ .

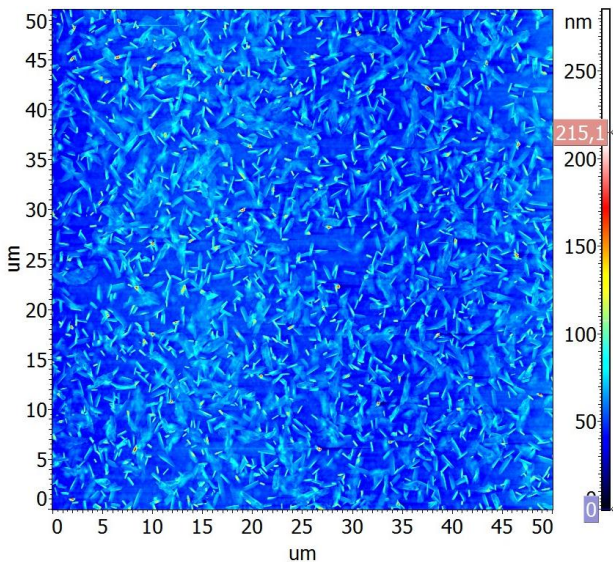


Figure 7: AFM surface morphology (scanned area  $50\times 50\text{ }\mu\text{m}$ ) of the roughest measurable layer prepared at  $T_S=360\text{ }^\circ\text{C}$  applying  $D_S=4\text{ Jcm}^{-2}$ .

## 4 CONCLUSION

The influence of the deposition conditions - the substrate temperature and laser beam density - on the quality of the surface (homogeneity and roughness) was analysed on thermoelectric nano layers prepared by PLD from  $\text{Bi}_2\text{Te}_3$  target. The smoothest layers were deposited at  $T_S=200\text{ }^\circ\text{C}$  while applying  $D_S=3\text{ Jcm}^{-2}$ . Such deposition conditions may not be optimal from thermoelectric properties point of view; because the layer stoichiometry is influenced by the deposition conditions. The measurement of thermoelectric properties has not been accomplished yet.

## 5 ACKNOWLEDGMENTS

The project has been supported by Czech Grant Agency under P108/13-33056S.

## REFERENCES

- [1] X.F. Tang, Q. Zhang, L. Chen, T. Goto, T. Hirai, J. Appl. Phys., 97, p. 093712, 2005.
- [2] B. C. Sales, D. Mandrus, B. C. Chakoumakos, V. Keppens, J. R. Thompson, Phys. Rev. B, 56, pp. 15081, 1997.
- [3] L. Jyun-Min, Ch. Ying-Chung, L. Chi-Pi, J. Nanomater., 201017, 2013.
- [4] S.X. Zhang, L. Yan, J. Qi, M. Zhuo, Y.-Q. Wang, R.P. Prasankumar, Q.X. Jia, S.T. Picarux, Thin. Sol. Films., 520, p. 6459, 2012.
- [5] Y. Zhenwei, W. Xiaolin, D. Yi, A. Sima, Z. Chao, Ch. Kris, L. Sean, J. Cryst. Growth., 362, p.247, 2013.
- [6] I.S. Virt, T.P. Shkumbatyuk, I.V. Kurilo, I.O. Rudyi, T.Ye. Lopatinskyi, L.F. Linnik, V.V. Tetyorkin, A.G. Phedorov, Semiconductors, 44, p. 544, 2010.
- [7] R. Zeipl, S. Karamazov, M. Jelinek, P. Lošťák, M. Pavelka, Sz. Winiarz, R. Czajka, J. Vaniš, F. Šroubek, J. Zelinka, J. Walachová, Proceedings of the 22<sup>nd</sup> International Conference on Thermoelectrics, La Grande Motte, France, August 17-21, p. 342, 2003.
- [8] J. Walachová, R. Zeipl, J. Zelinka, V. Malina, Appl. Phys. Lett., 87, p. 081902, 2005.